Crystalline Electric-Field Randomness in the Triangular Lattice Spin-Liquid $YbMgGaO_4$

Yuesheng Li,[1,2,*] Devashibhai Adroja,[3,4] Robert I. Bewley,[3] David Voneshen,[3]
Alexander A. Tsirlin,[2] Philipp Gegenwart,[2] and Qingming Zhang[1,5,6,†]
[1]*Department of Physics, Renmin University of China, Beijing 100872, People's Republic of China*
[2]*Experimental Physics VI, Center for Electronic Correlations and Magnetism, University of Augsburg, 86159 Augsburg, Germany*
[3]*ISIS Pulsed Neutron and Muon Source, STFC Rutherford Appleton Laboratory, Harwell Campus, Didcot, Oxfordshire, OX11 0QX, United Kingdom*
[4]*Highly Correlated Matter Research Group, Physics Department, University of Johannesburg, PO Box 524, Auckland Park 2006, South Africa*
[5]*Department of Physics and Astronomy, Shanghai Jiao Tong University, Shanghai 200240, People's Republic of China*
[6]*Collaborative Innovation Center of Advanced Microstructures, Nanjing 210093, People's Republic of China*
(Received 4 October 2016; revised manuscript received 1 December 2016; published 7 March 2017)

We apply moderate-high-energy inelastic neutron scattering (INS) measurements to investigate Yb^{3+} crystalline electric field (CEF) levels in the triangular spin-liquid candidate $YbMgGaO_4$. Three CEF excitations from the ground-state Kramers doublet are centered at the energies $\hbar\omega = 39$, 61, and 97 meV in agreement with the effective spin-1/2 g factors and experimental heat capacity, but reveal sizable broadening. We argue that this broadening originates from the site mixing between Mg^{2+} and Ga^{3+} giving rise to a distribution of Yb-O distances and orientations and, thus, of CEF parameters that account for the peculiar energy profile of the CEF excitations. The CEF randomness gives rise to a distribution of the effective spin-1/2 g factors and explains the unprecedented broadening of low-energy magnetic excitations in the fully polarized ferromagnetic phase of $YbMgGaO_4$, although a distribution of magnetic couplings due to the Mg/Ga disorder may be important as well.

DOI: 10.1103/PhysRevLett.118.107202

Introduction.—Quantum spin liquid (QSL) is a novel state of matter with zero entropy and without conventional symmetry breaking even at zero temperature. Such states were proposed to host "spinons," exotic spin excitations with fractional quantum numbers [1–3]. Although many candidate QSL materials with two-dimensional or three-dimensional interaction topologies on the triangular, kagome, and pyrochlore lattices were reported [4–17], they typically suffer from magnetic or nonmagnetic defects [18–22], spatial anisotropy [4,7,15], antisymmetric Dzyaloshinsky-Moriya anisotropy [23–25], and (or) interlayer magnetic couplings [25–27] that reduce or even completely release magnetic frustration [25,27–30].

Many of the aforementioned shortcomings can be remedied in a new triangular antiferromagnet $YbMgGaO_4$ that was recently reported by our group [31–33]. No spin freezing was detected down to at least 0.048 K, which is about 3% of the nearest-neighbor interaction $J_0 \sim 1.5$ K [33]. Residual spin entropy is nearly zero at 0.06 K, excluding any magnetic transitions at lower temperatures [31]. Below 0.4 K, thermodynamic properties evidence the putative QSL regime with temperature-independent magnetic susceptibility $\chi = \text{const}$ [33] and power-law behavior of the magnetic heat capacity, $C_m \sim T^{2/3}$ [31], the observations that are consistent with theoretical predictions for the U(1) QSL ground state (GS) on the triangular lattice [34–36].

Very recently, two inelastic neutron scattering (INS) studies of $YbMgGaO_4$ [37,38] reported continuous excitations at transfer energies of 0.1–2.5 meV extending well above the energy scale of the magnetic coupling $J_0 \sim 0.13$ meV. These spectral features were identified as fractionalized excitations (spinons) from the QSL GS [37]. Surprisingly, though, magnetic excitations remain very broad in both energy and wave vector (Q) even in the almost fully polarized state at 7.8 T, where only narrow spin-wave excitations of an ordered ferromagnet are expected [38]. This persistent broadening of magnetic excitations may be related to a very inconspicuous intrinsic structural disorder that we uncover and quantify by INS measurements at high energies, where crystalline electric field (CEF) excitations of Yb^{3+} ions can be probed.

In this Letter, we report a comprehensive investigation of the CEF excitations in $YbMgGaO_4$. They are observed at the energies of $\hbar\omega = 39$, 61, and 97 meV and show not only a pronounced broadening, but also a very peculiar energy profile with a shoulder around 87 meV on the side of the 97 meV excitation. These peculiarities are rationalized by considering the frozen Mg/Ga disorder that affects the local environment of Yb^{3+} and, thus, the CEF parameters. Their randomness gives rise to a distribution of electronic g factors and explains the broadening of low-energy magnetic excitations, thus rendering structural randomness an important ingredient of the QSL physics in $YbMgGaO_4$.

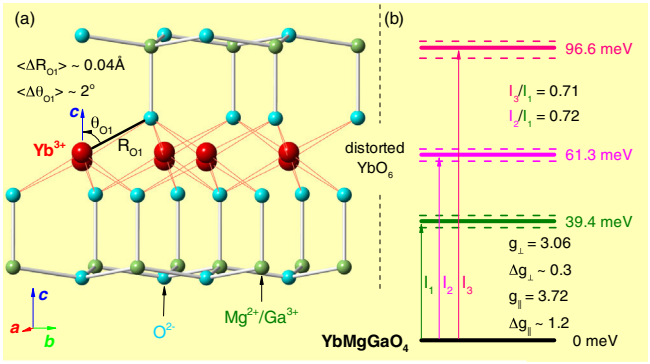

FIG. 1. (a) Crystal structure of $YbMgGaO_4$. The random distribution of Mg^{2+} and Ga^{3+} causes local distortions of the YbO_6 environments due to uneven charge distribution around the Yb^{3+} site [41]. (b) Four Kramers doublet energy levels and three CEF excitations obtained from the CEF fit. The dashed lines illustrate the broadening of the CEF excitations due to the inherent structural disorder.

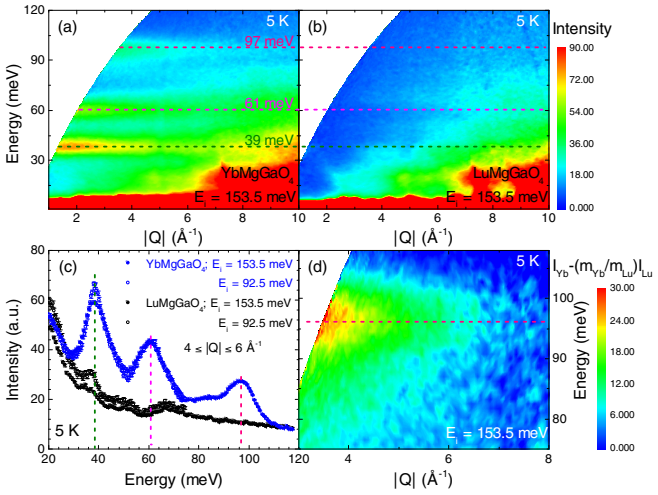

FIG. 2. MERLIN INS spectra for (a) $YbMgGaO_4$ and (b) $LuMgGaO_4$ measured with the incident neutron energy of 153.5 meV at 5 K. (c) Energy dependence of the INS intensity at 5 K for both $YbMgGaO_4$ and $LuMgGaO_4$ measured with different incident neutron energies. The data have been integrated over the wave vector space $4 \leq |Q| \leq 6$ Å^{-1}. Three CEF excitations of Yb^{3+} are highlighted by colored dashed lines. The INS intensities of $LuMgGaO_4$ are multiplied by m_{Yb}/m_{Lu}. (d) Zoom-in view of the CEF excitation around 97 meV.

Experimental technique.—Moderate-high-energy INS data and low-energy INS data were collected, respectively, on the MERLIN [39] and LET [40] spectrometers at the ISIS pulsed neutron facility, Rutherford Appleton Laboratory, U.K. [41]. Several incident energies E_i were used at MERLIN. In the following, we focus on the data obtained with $E_i = 153.5$ meV that provides the best trade-off between the resolution and energy coverage [53]. Our $YbMgGaO_4$ ($m_{Yb} = 14.03$ g) and $LuMgGaO_4$ ($m_{Lu} = 6.36$ g) powder samples for the MERLIN experiment were prepared using solid-state reactions [31]. Single crystals of $YbMgGaO_4$ for the LET experiment were grown by the floating zone technique [32].

CEF excitations.—According to the Hund's rules, the free Yb^{3+} ($4f^{13}$) ion has the spin angular momentum $s = 1/2$ and orbital angular momentum $L = 3$ resulting in the eightfold-degenerate ground state with the total angular momentum $J = 7/2$ and Landé g factor $g_J = 8/7$ for the GS multiplet. In the idealized $YbMgGaO_4$ structure, Yb^{3+} has trigonal local symmetry with the point group D_{3d} [see Fig. 1(a)] that splits this multiplet into four Kramers doublets [41] [see Fig. 1(b)].

Raw INS spectra for both $YbMgGaO_4$ and its nonmagnetic analog $LuMgGaO_4$ are shown in panels (a) and (b) of Fig. 2, respectively. Their comparison reveals three features that are identified as CEF excitations of Yb^{3+} based on the following observations. (i) These excitations are absent in the nonmagnetic reference compound $LuMgGaO_4$ [Fig. 2 (b)]. (ii) The lowest-lying excitation at around ~39.4 meV [see Fig. 2(c)] is consistent with the energy separation $\Delta \sim 36.5(1)$ meV between the ground-state Kramers doublet and the first excited state, as found in our previous heat capacity measurements [32]. (iii) No systematic anharmonic effect is observed, thus excluding the phonon origin of the excitations [41,54]. (iv) Q-independent excitation energies [see Fig. 2(a)] suggest their single-ion nature. (v) The intensities decrease with Q following the square of the magnetic form factor of the Yb^{3+} ion [see Fig. 3(b)]. (vi) The lowest excitation at around 39 meV is far above $J_0 \simeq 0.13$ meV and, therefore, unrelated to the spin-spin correlations in $YbMgGaO_4$. All these facts indicate that three spectral features are single-ion CEF excitations. For a Yb^{3+} ion with $J = 7/2$ in the D_{3d} symmetry, we indeed expect four CEF doublets and, thus, three CEF excitations from the ground-state doublet.

A closer inspection of these CEF excitations reveals two unusual features, though. First, all excitations are much broader than the instrumental resolution. For example, at $E_i = 153.5$ meV the total FWHMs (full width at half maximum obtained from the convoluted Lorentzian and Gaussian peak profiles) are 10.1(4) meV ($\hbar\omega_1 \sim 39$ meV), 10.9(4) meV ($\hbar\omega_2 \sim 61$ meV), and 12.2(7) meV ($\hbar\omega_3 \sim 97$ meV), much larger than the instrumental resolutions (Gaussian component) of 6.7, 5.6, and 4.3 meV, respectively. Through convolution calculations, we determine the additional broadening (Lorentzian component) of 5.5, 7.9, and 10.7 meV, respectively. Given the high quality of our sample [41] and the low temperature of the measurement ($T = 5$ K), we conclude that this broadening is intrinsic.

Another peculiar feature is the shape of the highest CEF excitation that shows the main peak around 97 meV and a shoulder at ~87 meV [see Fig. 2(d)]. The Q dependence of the intensity at ~87 meV follows the square of the magnetic form factor of the Yb^{3+} ion [41], thus proving the

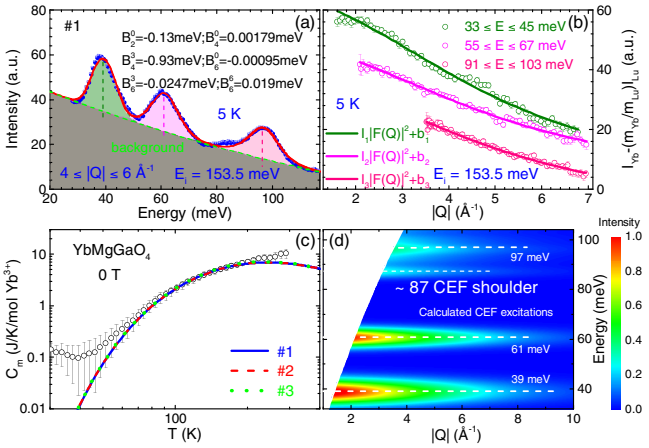

FIG. 3. (a) Peak fit to the INS spectra of $YbMgGaO_4$ (No. 1) at 5 K. Three peak centers are obtained (colored dashed lines). (b) Wave vector ($|Q|$) dependence of the INS intensities around the three CEF excitations. Lattice contributions are subtracted by the nonmagnetic counterpart $[(m_{Yb}/m_{Lu})I_{Lu}]$ measured on $LuMgGaO_4$. Colored curves show the fit with a small constant background [i.e., $I_k|F(Q)|^2 + b_k$] to the integrated INS data, where $I_k \gg |b_k|$. (c) Temperature dependence of the magnetic heat capacity measured on $YbMgGaO_4$ single crystals. Lattice contribution is subtracted using the heat capacity of $LuMgGaO_4$ [32]. The blue solid, red dashed, and green dotted curves show the calculated heat capacities using three series of the fitted CEF parameters (No. 1, No. 2, and No. 3) [41], respectively. (d) INS spectra calculated by considering different nearest-neighbor oxygen environments (distorted YbO_6 octahedra) [41] convoluted with the corresponding instrumental resolutions.

CEF origin of this spectral feature. It contributes about 40% of the overall intensity of the highest-energy excitation and is clearly intrinsic. Further, there are no phonon modes observed between ~70 and 120 meV in $LuMgGaO_4$ [see Fig. 2(b)] and, hence, the ~87 meV shoulder could not be due to CEF-phonon coupling [55].

Combined CEF fit.—To determine the CEF parameters, we fit energy dependence of the experimental intensity in three fashions [see Fig. 3(a) and Ref. [41]]. Fit No. 1 is performed against the whole data set [see Fig. 3(a)]. For fit No. 2 we excluded the region between 73 and 90 meV, where the additional shoulder is observed, while fit No. 3 is performed against the whole data set with a four-peaks fit and uses the additional shoulder energy (~87 meV) as $\hbar\omega_3$. All fits share the same measured relative INS intensities, I_2/I_1 and I_3/I_1 [see Fig. 3(b)], and the same measured effective spin-1/2 g factors [32]. Through combined fits to these seven observables—$\hbar\omega_1$, $\hbar\omega_2$, $\hbar\omega_3$, I_2/I_1, I_3/I_1, $g_\perp$, and $g_\parallel$—we obtain all six CEF parameters B_n^m [41] by minimizing the following deviation function,

$$R_p = \sqrt{\frac{1}{7}\sum_{i=1}^{7}\left(\frac{X_i^{\mathrm{obs}} - X_i^{\mathrm{cal}}}{\sigma_i^{\mathrm{obs}}}\right)^2}, \qquad (1)$$

where X_i^{obs} and σ_i^{obs} are the experimental value and its standard deviation, respectively, whereas X_i^{cal} is the calculated value. Qualitatively similar CEF parameters and wave functions are found from fits No. 1, No. 2, and No. 3, as shown in Ref. [41], respectively. The magnetic part of the experimental heat capacity (C_m) is very well reproduced [see Fig. 3(c)]:

$$C_m^{\mathrm{CEF}} = \frac{1}{k_B T^2}\frac{\partial^2 \ln[\sum_{k=0}^{3} 2\exp(-\frac{\hbar\omega_k}{k_B T})]}{\partial(\frac{1}{k_B T})^2}. \qquad (2)$$

Inherent structural disorder and CEF randomness.—The peculiar shape of the CEF excitations is rooted in subtle details of the $YbMgGaO_4$ crystal structure. Our single-crystal x-ray diffraction study excludes any global symmetry reduction or a site mixing between Yb and Mg/Ga [41]. On the other hand, Mg and Ga share one crystallographic site, thus forming different local configurations around each Yb^{3+} ion. The most obvious effect of this Mg/Ga disorder is the variation of the electrostatic potential imposed on Yb^{3+}. We assess it by calculating CEF parameters using the point-charge model [41] and find that as long as Yb occupies its ideal position at (0,0,0), the random distribution of Mg and Ga gives rise to only a weak broadening of the CEF excitations, $\Delta(\hbar\omega_1) = 0.27$ meV, $\Delta(\hbar\omega_2) = 0.26$ meV, and $\Delta(\hbar\omega_3) = 0.39$ meV, and does not account for our experimental observations. Moreover, all three CEF excitations remain symmetric.

A further effect of the Mg/Ga disorder is local charge misbalance that may push Yb out of its ideal position, as reflected by the enhanced values of the Yb atomic displacement parameter, with the thermal ellipsoid elongated along the c direction [41,56]. We probed this effect quantitatively by constructing several representative Mg/Ga configurations and optimizing their geometry using density-functional calculations [41]. We indeed observed that exact positions of both Yb and its neighboring oxygens are affected by the local distribution of Mg^{2+} and Ga^{3+}. The resulting distortions of the YbO_6 octahedra give rise to a pronounced distribution of the CEF parameters and render the highest-lying CEF excitation asymmetric [41]. Both the ~87 meV shoulder and the overall broadening of the CEF excitations can be well reproduced [see Fig. 3(d) and Ref. [41]]. Consequently, the effective spin-1/2 g factors show a maximum distribution as follows: $\Delta g_\perp \sim 0.3$ and $\Delta g_\parallel \sim 1.2$ [41]. This distribution of the g values has immediate ramifications for low-energy excitations, as we show below. Eventually, intersite magnetic couplings should be random too [57], although perhaps in a more complicated manner.

Prior to discussing the low-energy excitations, let us note that the broadening of CEF excitations is not uncommon for rare-earth compounds [58–60]. This effect is usually ascribed to antisite defects, as in the "stuffed"' quantum

spin ice, $Yb_2Ti_{2-x}Yb_xO_{7-x/2}$ with $x \sim 0.01-0.02$ [57,61,62]. On the other hand, site mixing beyond the rare-earth site, as in $Tb_2Sn_{2-x}Ti_xO_7$, is believed to merge the CEF excitations into a broad continuum [63]. Interestingly, $YbMgGaO_4$ with its complete Mg/Ga disorder and *without* any detectable Yb antisite defects retains well-defined CEF excitations, albeit with a peculiar energy profile that can be reproduced, perhaps for the first time, by considering local atomic relaxation depending on the distribution of Mg and Ga around Yb^{3+}.

Spin-wave continuum.—Under the field of 8.5 T applied along the c axis, the spin system is fully polarized according to the static magnetization measurement at 1.9 K [41]. Therefore, at 8.5 T and 0.1 K the fully polarized (ferromagnetic) state should give rise to narrow spin-wave excitations having the width of about 0.16 meV according to the instrumental resolution of LET. In contrast, the measured INS signals are still broadly distributed in the energy space with a width of more than 0.5 meV [see Fig. 4 (a)]. This width is obviously larger than the instrumental resolution [40] and than the width of spin-wave excitations in single crystals of a similar Yb^{3+} material, $Yb_2Ti_2O_7$ [17]. Similarly broad excitations were

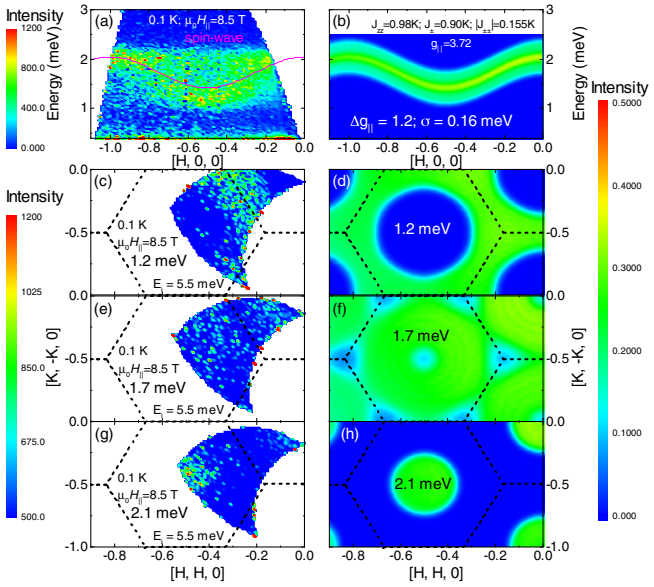

FIG. 4. LET INS spectra of a $YbMgGaO_4$ single crystal sample measured at 0.1 K under a field of 8.5 T applied along the c axis, the incident neutron energy is 5.5 meV. (a) Energy dependence of the excitations along the wave vector direction $[H, 0, 0]$. (c),(e), and (g) Wave vector dependence of the excitations at the transfer energies 1.2, 1.7, and 2.1 meV, respectively. (b),(d),(f), and (h) Calculated spin-wave excitations using the previously reported effective spin-1/2 g factor and coupling constants [32] by considering a convolution of the broadening of $g_{\|}$ ($\Delta g_{\|} = 1.2$) and the instrumental Gaussian broadening ($\sigma = 0.16$ meV). The calculated spin-wave dispersion without any broadening is shown in (a) (pink line). The black dashed lines represent Brillouin zone boundaries.

observed in the recent INS measurement performed in the applied field of 7.8 T at 0.06 K [38]. Our magnetization data [41] confirm that at 8.5 T the Yb^{3+} spins are fully polarized along the c axis. Nevertheless, the excitations remain very broad. Thus, the natural explanation to this observed spin-wave continuum is the aforementioned randomness of the effective spin-1/2 g factors and (or) couplings, since linear spin-wave theory should be applicable to $YbMgGaO_4$ at 8.5 T and 0.1 K.

We model the spin-wave excitations in the ab plane under the high applied field along the c axis using the expression [64]

$$\frac{d^2\sigma}{d\Omega d\omega} \propto |F(|\mathbf{Q}|)|^2 \times \left(\frac{Q_y^2 S^{xx}(\mathbf{Q}, E) + Q_x^2 S^{yy}(\mathbf{Q}, E)}{|\mathbf{Q}|^2} + S^{zz}(\mathbf{Q}, E) \right), \quad (3)$$

where $F(|\mathbf{Q}|)$ is the magnetic form factor of Yb^{3+} and $S^{\alpha\alpha}(\mathbf{Q}, E)$ ($\alpha = x$, y, or z) is the dynamic spin structure factor calculated by the Spinw-Matlab code based on the linear spin-wave theory [65–67] and coupling parameters reported earlier [32]. By considering the maximum broadening of $g_{\|}$, $\Delta g_{\|} = 1.2$, and the instrumental Gaussian broadening, $\sigma = 0.16$ meV, we are able to reproduce the broadening of about 0.7 meV at the zone center. However, the signal is even broader at the zone boundary. While the on-site randomness is clearly very important for the low-energy physics, a distribution of magnetic couplings is relevant too and requires further investigation.

Conclusions.—The CEF excitations of Yb^{3+} in the triangular QSL $YbMgGaO_4$ have been studied by moderate-high-energy INS measurements. Large broadening and peculiar energy profile of the CEF excitations is observed and ascribed to the structural randomness, namely, the random distribution of Mg and Ga that affects local coordination of the Yb^{3+} ions. We propose that this inherent structural disorder results in the distribution of the effective spin-1/2 g factors, which, in turn, is responsible for the persistent broadening of low-energy magnetic excitations in the fully polarized ferromagnetic state, although the distribution of magnetic couplings seems to be relevant too. Our results put forward structural randomness as an important ingredient in the spin-liquid physics, an observation that goes hand in hand with the recent report on the suppression of thermal conductivity at low temperatures [68]. In $4f$-based materials, the randomness of CEF levels can be easily introduced without generating strong structural disorder, thus opening interesting prospects for the design of new spin-liquid materials [69].

We thank Jinchen Wang and Yu Li for helpful discussion. Y. L. thanks Duc Le for introducing him to the Mantid (3.7.1) software for CEF fits. A. T. acknowledges Tom Fennell for pointing our recent examples of CEF

excitations broadening. This work was supported by the NSF of China (No. 11474357) and the Ministry of Science and Technology of China (973 Projects No. 2016YFA0300504). Y. S. L. was supported by the start-up funds of Renmin University of China. The work in Augsburg was supported by the German Federal Ministry for Education and Research through the Sofja Kovalevskaya Award of Alexander von Humboldt Foundation. Q. M. Z. was supported by the Fundamental Research Funds for the Central Universities, and by the Research Funds of Renmin University of China.

Note added.—After the submission of our Letter, the results of Ref. [38] were updated as it progressed from a preprint to a published article incorporating high-energy INS data that are largely consistent with our results.

*yuesheng.man.li@gmail.com
†qmzhang@ruc.edu.cn

[1] L. Balents, Spin liquids in frustrated magnets, Nature (London) **464**, 199 (2010).
[2] P. A. Lee, An end to the drought of quantum spin liquids, Science **321**, 1306 (2008).
[3] X.-G. Wen, *Quantum Field Theory of Many-Body Systems: From the Origin of Sound to an Origin of Light and Electrons* (Oxford University Press on Demand, Oxford, 2004).
[4] Y. Shimizu, K. Miyagawa, K. Kanoda, M. Maesato, and G. Saito, Spin Liquid State in an Organic Mott Insulator with A Triangular Lattice, Phys. Rev. Lett. **91**, 107001 (2003).
[5] S. Yamashita, Y. Nakazawa, M. Oguni, Y. Oshima, H. Nojiri, Y. Shimizu, K. Miyagawa, and K. Kanoda, Thermodynamic properties of a spin-1/2 spin-liquid state in a κ-type organic salt, Nat. Phys. **4**, 459 (2008).
[6] M. Yamashita, N. Nakata, Y. Kasahara, T. Sasaki, N. Yoneyama, N. Kobayashi, S. Fujimoto, T. Shibauchi, and Y. Matsuda, Thermal-transport measurements in a quantum spin-liquid state of the frustrated triangular magnet κ-$(BEDT\text{-}TTF)_2Cu_2(CN)_3$, Nat. Phys. **5**, 44 (2009).
[7] T. Itou, A. Oyamada, S. Maegawa, M. Tamura, and R. Kato, Quantum spin liquid in the spin-1/2 triangular antiferromagnet $EtMe_3Sb[Pd(dmit)_2]_2$, Phys. Rev. B **77**, 104413 (2008).
[8] T. Itou, A. Oyamada, S. Maegawa, and R. Kato, Instability of a quantum spin liquid in an organic triangular-lattice antiferromagnet, Nat. Phys. **6**, 673 (2010).
[9] S. Yamashita, T. Yamamoto, Y. Nakazawa, M. Tamura, and R. Kato, Gapless spin liquid of an organic triangular compound evidenced by thermodynamic measurements, Nat. Commun. **2**, 275 (2011).
[10] M. P. Shores, E. A. Nytko, B. M. Bartlett, and D. G. Nocera, A structurally perfect $S = 1/2$ kagome antiferromagnet, J. Am. Chem. Soc. **127**, 13462 (2005).
[11] T. H. Han, J. S. Helton, S. Chu, D. G. Nocera, J. A. Rodriguez-Rivera, C. Broholm, and Y. S. Lee, Fractionalized excitations in the spin-liquid state of a kagome-lattice antiferromagnet, Nature (London) **492**, 406 (2012).
[12] M. Fu, T. Imai, T. H. Han, and Y. S. Lee, Evidence for a gapped spin-liquid ground state in a kagome Heisenberg antiferromagnet, Science **350**, 655 (2015).
[13] B. Fåk, E. Kermarrec, L. Messio, B. Bernu, C. Lhuillier, F. Bert, P. Mendels, B. Koteswararao, F. Bouquet, J. Ollivier, A. D. Hillier, A. Amato, R. H. Colman, and A. S. Wills, Kapellasite: A Kagome Quantum Spin Liquid with Competing Interactions, Phys. Rev. Lett. **109**, 037208 (2012).
[14] L. Clark, J. C. Orain, F. Bert, M. A. De Vries, F. H. Aidoudi, R. E. Morris, P. Lightfoot, J. S. Lord, M. T. F. Telling, P. Bonville, J. P. Attfield, P. Mendels, and A. Harrison, Gapless Spin Liquid Ground State in the $S=1/2$ Vanadium Oxyfluoride Kagome Antiferromagnet $[NH_4]_2[C_7H_{14}N][V_7O_6F_{18}]$, Phys. Rev. Lett. **110**, 207208 (2013).
[15] Y. Li, B. Pan, S. Li, W. Tong, L. Ling, Z. Yang, J. Wang, Z. Chen, Z. Wu, and Q. Zhang, Gapless quantum spin liquid in the $S = 1/2$ anisotropic kagome antiferromagnet $ZnCu_3(OH)_6SO_4$, New J. Phys. **16**, 093011 (2014).
[16] J. A. Hodges, P. Bonville, A. Forget, A. Yaouanc, P. Dalmas de Réotier, G. André, M. Rams, K. Królas, C. Ritter, P. C. M. Gubbens, C. T. Kaiser, P. J. C. King, and C. Baines, First-Order Transition in the Spin Dynamics of Geometrically Frustrated $Yb_2Ti_2O_7$, Phys. Rev. Lett. **88**, 077204 (2002).
[17] K. A. Ross, L. Savary, B. D. Gaulin, and L. Balents, Quantum excitations in quantum spin ice, Phys. Rev. X **1**, 021002 (2011).
[18] S. H. Lee, H. Kikuchi, Y. Qiu, B. Lake, Q. Huang, K. Habicht, and K. Kiefer, Quantum-spin-liquid states in the two-dimensional kagome antiferromagnets $Zn_xCu_{4-x}(OD)_6Cl_2$, Nat. Mater. **6**, 853 (2007).
[19] D. E. Freedman, T. H. Han, A. Prodi, P. Müller, Q. Z. Huang, Y. S. Chen, S. M. Webb, Y. S. Lee, T. M. McQueen, and D. G. Nocera, Site specific x-ray anomalous dispersion of the geometrically frustrated kagome magnet, herbertsmithite, $ZnCu_3(OH)_6Cl_2$, J. Am. Chem. Soc. **132**, 16185 (2010).
[20] Y. Li and Q. Zhang, Structure and magnetism of $S = \frac{1}{2}$ kagome antiferromagnets $NiCu_3(OH)_6Cl_2$ and $CoCu_3(OH)_6Cl_2$, J. Phys. Condens. Matter **25**, 026003 (2013).
[21] Y. Li, J. Fu, Z. Wu, and Q. Zhang, Transition-metal distribution in kagome antiferromagnet $CoCu_3(OH)_6Cl_2$ revealed by resonant x-ray diffraction, Chem. Phys. Lett. **570**, 37 (2013).
[22] M. Gomilšek, M. Klanjšek, M. Pregelj, H. Luetkens, Y. Li, Q. M. Zhang, and A. Zorko, μSR insight into the impurity problem in quantum kagome antiferromagnets, Phys. Rev. B **94**, 024438 (2016).
[23] T. Moriya, New Mechanism of Anisotropic Superexchange Interaction, Phys. Rev. Lett. **4**, 228 (1960).
[24] A. Zorko, S. Nellutla, J. van Tol, L. C. Brunel, F. Bert, F. Duc, J. C. Trombe, M. A. de Vries, A. Harrison, and P. Mendels, Dzyaloshinsky-Moriya Anisotropy in the Spin-1/2 Kagome Compound $ZnCu_3(OH)_6Cl_2$, Phys. Rev. Lett. **101**, 026405 (2008).
[25] N. A. Fortune, S. T. Hannahs, Y. Yoshida, T. E. Sherline, T. Ono, H. Tanaka, and Y. Takano, Cascade of Magnetic-Field-Induced Quantum Phase Transitions in A Spin-$\frac{1}{2}$ Triangular-Lattice Antiferromagnet, Phys. Rev. Lett. **102**, 257201 (2009).

[26] Y. Doi, Y. Hinatsu, and K. Ohoyama, Structural and magnetic properties of pseudo-two-dimensional triangular antiferromagnets $Ba_3MSb_2O_9$ (M = Mn, Co, and Ni), J. Phys. Condens. Matter **16**, 8923 (2004).

[27] Y. Shirata, H. Tanaka, A. Matsuo, and K. Kindo, Experimental Realization of a Spin-1/2 Triangular-Lattice Heisenberg Antiferromagnet, Phys. Rev. Lett. **108**, 057205 (2012).

[28] S. Dommange, M. Mambrini, B. Normand, and F. Mila, Static impurities in the $S = 1/2$ kagome lattice: Dimer freezing and mutual repulsion, Phys. Rev. B **68**, 224416 (2003).

[29] M. Rigol and R. R. P. Singh, Magnetic Susceptibility of the Kagome Antiferromagnet $ZnCu_3(OH)_6Cl_2$, Phys. Rev. Lett. **98**, 207204 (2007).

[30] I. Rousochatzakis, S. R. Manmana, A. M. Läuchli, B. Normand, and F. Mila, Dzyaloshinskii-Moriya anisotropy and nonmagnetic impurities in the $s = \frac{1}{2}$ kagome system $ZnCu_3(OH)_6Cl_2$, Phys. Rev. B **79**, 214415 (2009).

[31] Y. Li, H. Liao, Z. Zhang, S. Li, F. Jin, L. Ling, L. Zhang, Y. Zou, L. Pi, Z. Yang *et al.*, Gapless quantum spin liquid ground state in the two-dimensional spin-1/2 triangular antiferromagnet $YbMgGaO_4$, Sci. Rep. **5**, 16419 (2015).

[32] Y. Li, G. Chen, W. Tong, L. Pi, J. Liu, Z. Yang, X. Wang, and Q. Zhang, Rare-Earth Triangular Lattice Spin Liquid: A Single-Crystal Study of $YbMgGaO_4$, Phys. Rev. Lett. **115**, 167203 (2015).

[33] Y. Li, D. Adroja, P. K. Biswas, P. J. Baker, Q. Zhang, J. Liu, A. A. Tsirlin, P. Gegenwart, and Q. Zhang, Muon Spin Relaxation Evidence for the U(1) Quantum Spin-Liquid Ground State in the Triangular Antiferromagnet $YbMgGaO_4$, Phys. Rev. Lett. **117**, 097201 (2016).

[34] O. I. Motrunich, Variational study of triangular lattice spin-$\frac{1}{2}$ model with ring exchanges and spin liquid state in κ-$(ET)_2Cu_2(CN)_3$, Phys. Rev. B **72**, 045105 (2005).

[35] S. S. Lee and P. A. Lee, U(1) Gauge Theory of the Hubbard Model: Spin Liquid States And Possible Application to k-$(BEDT\text{-}TTF)_2Cu_2(CN)_3$, Phys. Rev. Lett. **95**, 036403 (2005).

[36] O. I. Motrunich, Orbital magnetic field effects in spin liquid with spinon Fermi sea: Possible application to κ-$(ET)_2Cu_2(CN)_3$, Phys. Rev. B **73**, 155115 (2006).

[37] Y. Shen, Y. Li, H. Wo, Y. Li, S. Shen, B. Pan, Q. Wang, H. C. Walker, P. Steffens, M. Boehm, Y. Hao, D. L. Quintero-Castro, L. W. Harriger, M. D. Frontzek, L. Hao, S. Meng, Q. Zhang, G Chen, and J. Zhao, Evidence for a spinon Fermi surface in a triangular-lattice quantum-spin-liquid candidate, Nature (London) **540**, 559 (2016).

[38] J. A. M. Paddison, M. Daum, Z. Dun, G. Ehlers, Y. Liu, M. B. Stone, H. Zhou, and M. Mourigal, Continuous excitations of the triangular-lattice quantum spin liquid $YbMgGaO_4$, Nat. Phys. **13**, 117 (2017).

[39] R. I. Bewley, R. S. Eccleston, K. A. McEwen, S. M. Hayden, M. T. Dove, S. M. Bennington, J. R. Treadgold, and R. L. S. Coleman, MERLIN, a new high count rate spectrometer at ISIS, Physica B (Amsterdam) **385B**, 1029 (2006).

[40] R. I. Bewley, J. W. Taylor, and S. M. Bennington, LET, a cold neutron multi-disk chopper spectrometer at ISIS, Nucl. Instrum. Methods Phys. Res., Sect. A **637**, 128 (2011).

[41] See Supplemental Material at http://link.aps.org/supplemental/10.1103/PhysRevLett.118.107202 for detailed information about experimental procedures, which includes Refs. [42–52].

[42] A. Bertin, Y. Chapuis, P. D. de Réotier, and A. Yaouanc, Crystal electric field in the $R_2Ti_2O_7$ pyrochlore compounds, J. Phys. Condens. Matter **24**, 256003 (2012).

[43] I. Mirebeau, P. Bonville, and M. Hennion, Magnetic excitations in $Tb_2Sn_2O_7$ and $Tb_2Ti_2O_7$ as measured by inelastic neutron scattering, Phys. Rev. B **76**, 184436 (2007).

[44] M. Ruminy, E. Pomjakushina, K. Iida, K. Kamazawa, D. T. Adroja, U. Stuhr, and T. Fennell, Crystal-field parameters of the rare-earth pyrochlores $R_2Ti_2O_7$ (R = Tb, Dy, and Ho), Phys. Rev. B **94**, 024430 (2016).

[45] A. Furrer, P. Brüesch, and P. Unternährer, Neutron spectroscopic determination of the crystalline electric field in $HoBa_2Cu_3O_{7-\delta}$, Phys. Rev. B **38**, 4616 (1988).

[46] C. Mazumdar, M. Rotter, M. Frontzek, H. Michor, M. Doerr, A. Kreyssig, M. Koza, A. Hiess, J. Voigt, G. Behr, L. C. Gupta, M. Prager, and M. Loewenhaupt, Crystalline electric field effects in $PrNi_2B_2C$: Inelastic neutron scattering, Phys. Rev. B **78**, 144422 (2008).

[47] S. Chi, D. T. Adroja, T. Guidi, R. Bewley, S. Li, J. Zhao, J. W. Lynn, C. M. Brown, Y. Qiu, G. F. Chen, J. L. Lou, N. L. Wang, and P. Dai, Crystalline Electric Field as a Probe for Long-Range Antiferromagnetic Order and Superconducting State of $CeFeAsO_{1-X}F_X$, Phys. Rev. Lett. **101**, 217002 (2008).

[48] J. J. Baldoví, S. Cardona-Serra, J. M. Clemente-Juan, E. Coronado, A. Gaita-Ariño, and A. Palii, SIMPRE: A software package to calculate crystal field parameters, energy levels, and magnetic properties on mononuclear lanthanoid complexes based on charge distributions, J. Comput. Chem. **34**, 1961 (2013).

[49] S. K. Misra and S. Isber, EPR of the Kramers ions Er^{3+}, Nd^{3+}, Yb^{3+} and Ce^{3+} in $Y(NO_3)_3 \cdot 6H_2O$ and $Y_2(SO_4)_3 \cdot 8H_2O$ single crystals:: Study of hyperfine transitions, Physica B (Amsterdam) **253B**, 111 (1998).

[50] G. Kresse and J. Furthmüller, Efficiency of ab-initio total energy calculations for metals and semiconductors using a plane-wave basis set, Comput. Mater. Sci. **6**, 15 (1996).

[51] G. Kresse and J. Furthmüller, Efficient iterative schemes for *ab initio* total-energy calculations using a plane-wave basis set, Phys. Rev. B **54**, 11169 (1996).

[52] J. P. Perdew, K. Burke, and M. Ernzerhof, Generalized Gradient Approximation Made Simple, Phys. Rev. Lett. **77**, 3865 (1996).

[53] Note that the data obtained with $E_i = 307$ meV extend to much higher energies and reveal a weak excitation, presumably of CEF origin, at 139 meV. This feature has only 20% of the intensity of the 97 meV excitation and is likely due to a multiple scattering excitation, see Supplemental Material [41] for details.

[54] M. Balkanski, R. F. Wallis, and E. Haro, Anharmonic effects in light scattering due to optical phonons in silicon, Phys. Rev. B **28**, 1928 (1983).

[55] D. T. Adroja, A. del Moral, C. de la Fuente, A. Fraile, E. A. Goremychkin, J. W. Taylor, A. D. Hillier, and F. Fernandez-Alonso, Vibron Quasibound State in the

Noncentrosymmetric Tetragonal Heavy-Fermion Compound $CeCuAl_3$, Phys. Rev. Lett. **108**, 216402 (2012).

[56] R. J. Cava, A. P. Ramirez, Q. Huang, and J. J. Krajewski, Compounds with the $YbFe_2O_4$ structure type: frustrated magnetism and spin-glass behavior, J. Solid State Chem. **140**, 337 (1998).

[57] K. A. Ross, Th. Proffen, H. A. Dabkowska, J. A. Quilliam, L. R. Yaraskavitch, J. B. Kycia, and B. D. Gaulin, Lightly stuffed pyrochlore structure of single-crystalline $Yb_2Ti_2O_7$ grown by the optical floating zone technique, Phys. Rev. B **86**, 174424 (2012).

[58] A. J. Princep, H. C. Walker, D. T. Adroja, D. Prabhakaran, and A. T. Boothroyd, Crystal field states of Tb^{3+} in the pyrochlore spin liquid $Tb_2Ti_2O_7$ from neutron spectroscopy, Phys. Rev. B **91**, 224430 (2015).

[59] P. Babkevich, A. Finco, M. Jeong, B. Dalla Piazza, I. Kovacevic, G. Klughertz, K. W. Krämer, C. Kraemer, D. T. Adroja, E. Goremychkin, T. Unruh, T. Strässle, A. Di Lieto, J. Jensen, and H. M. Rønnow, Neutron spectroscopic study of crystal-field excitations and the effect of the crystal field on dipolar magnetism in $LiRF_4$ (R = Gd, Ho, Er, Tm, and Yb), Phys. Rev. B **92**, 144422 (2015).

[60] J. J. Wen, S. M. Koohpayeh, K. A. Ross, B. A. Trump, T. M. McQueen, K. Kimura, S. Nakatsuji, Y. Qiu, D. M. Pajerowski, J. R. D. Copley, and C. L. Broholm, A disordered route to the coulomb quantum spin liquid: Random transverse fields on spin ice in $Pr_2Zr_2O_7$, arXiv:1609.08551.

[61] J. Gaudet, D. D. Maharaj, G. Sala, E. Kermarrec, K. A. Ross, H. A. Dabkowska, A. I. Kolesnikov, G. E. Granroth, and B. D. Gaulin, Neutron spectroscopic study of crystalline electric field excitations in stoichiometric and lightly stuffed $Yb_2Ti_2O_7$, Phys. Rev. B **92**, 134420 (2015).

[62] J. Gaudet, K. A. Ross, E. Kermarrec, N. P. Butch, G. Ehlers, H. A. Dabkowska, and B. D. Gaulin, Gapless quantum excitations from an icelike splayed ferromagnetic ground state in stoichiometric $Yb_2Ti_2O_7$, Phys. Rev. B **93**, 064406 (2016).

[63] B. D. Gaulin, E. Kermarrec, M. L. Dahlberg, M. J. Matthews, F. Bert, J. Zhang, P. Mendels, K. Fritsch, G. E. Granroth, P. Jiramongkolchai, A. Amato, C. Baines, R. J. Cava, and P. Schiffer, Quenched crystal-field disorder and magnetic liquid ground states in $Tb_2Sn_{2-x}Ti_xO_7$, Phys. Rev. B **91**, 245141 (2015).

[64] G. Xu, Z. Xu, and J. M. Tranquada, Absolute cross-section normalization of magnetic neutron scattering data, Rev. Sci. Instrum. **84**, 083906 (2013).

[65] S. Toth and B. Lake, Linear spin wave theory for single-q incommensurate magnetic structures, J. Phys. Condens. Matter **27**, 166002 (2015).

[66] Y. Li, X. Wang, and G. Chen, Anisotropic spin model of strong spin-orbit-coupled triangular antiferromagnets, Phys. Rev. B **94**, 035107 (2016).

[67] Y.-D. Li, Y. Shen, Y. Li, J. Zhao, and G. Chen, The effect of spin-orbit coupling on the effective-spin correlation in $YbMgGaO_4$, arXiv:1608.06445.

[68] Y. Xu, J. Zhang, Y. S. Li, Y. J. Yu, X. C. Hong, Q. M. Zhang, and S. Y. Li, Absence of Magnetic Thermal Conductivity in the Quantum Spin-Liquid Candidate $YbMgGaO_4$, Phys. Rev. Lett. **117**, 267202 (2016).

[69] M. B. Sanders, F. A. Cevallos, and R. J. Cava, Magnetism in the $KBaRE(BO_3)_2$ (RE = Sm, Eu, Gd, Tb, Dy, Ho, Er, Tm, Yb, Lu) series: materials with a triangular rare earth lattice, arXiv:1611.08548.